

This is a provisional PDF only. Copyedited and fully formatted version will be made available soon.



ISSN: 0015-5659

e-ISSN: 1644-3284

Variation of the stapes and its surrounding anatomical structures based on micro-computed tomography

Authors: Li Gong, Yiwei Feng, Xianglong Tang, Wenwen Zhou, Songhua Tan, Anzhou Tang

DOI: 10.5603/FM.a2023.0056

Article type: Original article

Submitted: 2023-04-21

Accepted: 2023-07-29

Published online: 2023-08-04

This article has been peer reviewed and published immediately upon acceptance. It is an open access article, which means that it can be downloaded, printed, and distributed freely, provided the work is properly cited.

Articles in "Folia Morphologica" are listed in PubMed.

Variation of the stapes and its surrounding anatomical structures based on micro-computed tomography

Li Gong et al., Variation of the stapes structures

Li Gong, Yiwei Feng, Xianglong Tang, Wenwen Zhou, Songhua Tan, Anzhou Tang
First Affiliated Hospital of Guangxi Medical University, Nanning, China

Address for correspondence: Anzhou Tang, First Affiliated Hospital of Guangxi Medical University, Nanning 530000, China, e-mail: anzhoutang@foxmail.com

ABSTRACT

Background: Stapedotomy is the most efficient treatment for otosclerosis. The anatomical structure of the operation area is complex, but it has a great impact on the postoperative effect. We measure the anatomical parameters of the stapes and its surrounding structures to provide an anatomical reference for stapes surgery in otosclerosis.

Materials and methods: Fifteen adult cadaver heads (30 samples) were scanned using micro-CT. The stapes, facial nerve and external auditory canal were reconstructed by image processing. The stapes parameters and relationships between the stapes and surrounding structures were measured using a three-dimensional reconstruction model.

Results: The length, width and thickness of the stapes footplate were 2.93 ± 0.17 mm, 1.46 ± 0.08 mm and 0.30 ± 0.11 mm, respectively. The distance between the stapes footplate and long process of the incus was 3.79 ± 0.39 mm. The angle of the incudostapedial joint was $88.29 \pm 11.58^\circ$. The distance from the center of the stapes footplate to the facial canal was 1.60 ± 0.34 mm. In simulated stapes surgery, the minimum depth of the external auditory canal to be removed was 2.17 ± 0.91 mm, and no significant difference was found between the left and right sides and between men and women ($P > 0.05$).

Conclusions: A three-dimensional model of the stapes bone and its surrounding anatomical structures was established based on Micro-CT imaging. Anatomical parameters of the stapes bone and its surrounding structures were measured using the model. In stapedotomy, the

implanted piston diameter should be around 0.6mm, with a length of approximately 4.6mm. Care should be taken to protect the facial nerve canal during the surgery. These data provide reference for otologists.

Key words: stapes, stapes surgery, micro-CT, 3D reconstruction

INTRODUCTION

In 1704, Professor Valsalva found that stapes fixation is a cause of hearing loss. In 1841, Toynbee found 39 cases of stapes fixation after dissecting 1659 temporal bone specimens and confirmed that fixation of the stapes and vestibular window is a common cause of hearing loss(1). The pathogenesis of otosclerosis remains unclear. Its pathological manifestations are normal bone resorption in the primary osseous labyrinth, accompanied by cavernous transformation with abundant blood vessels(2). Lesions around the vestibular window and stapes footplate can fix the stapes and lead to conductive deafness, called stapes otosclerosis. Lesions invading the cochlea, semicircular canal or internal auditory canal cause inner ear damage, such as vertigo or sensorineural hearing loss, called cochlear otosclerosis; however, stapes otosclerosis is more common in the clinic(3).

Patients with otosclerosis can have affected quality of life because of hearing loss. Presently, many studies have shown that some drugs for patients in the early stage of otosclerosis can delay the disease and prevent deterioration(4). However, stapes surgery remains the most effective and commonly used method to improve the hearing of patients with otosclerosis. Over the past 60 years, stapes surgery has progressed through the development of the stapes mobilization era, semicircular canal fenestration era, and stapedectomy era, among others(5). Finally, stapedotomy has become the most commonly used standard surgical procedure to treat otosclerosis because of its lower surgical risk, better surgical outcomes, and fewer postoperative complications(6).

The structure of the middle ear and inner ear is subtle and complex, the space is narrow, and anatomical variation exists among individual patients(7). Therefore, clarifying the variation of the stapes and its surrounding structures in a preoperative evaluation before

stapes surgery is crucial. Presently, many reports have investigated the complex anatomical structure of the temporal bone, but few have focused on the spatial measurement of various anatomical relationships of the middle ear and inner ear through the external auditory canal path(8, 9). Additionally, the traditional process of measuring inner and middle ear anatomical structures is complex, and showing the spatial relationships through conventional dissection and sectioning is challenging, easily leading to measurement errors(10). Therefore, a detailed understanding of the anatomical characteristics of the region and spatial relationships of the components, as well as quantification of these data for some important structures, can provide a reference to select the surgical strategy and reduce the difficulty and risk of the operation.

Microcomputed tomography (micro-CT) is considered more appropriate to study 3D bone structures and microstructural changes(11). In this method, an X-ray source and detector are used to obtain 2D images of samples that can be combined to create a 3D reconstruction. It is a nondestructive, noninvasive imaging technology with a high spatial resolution. Additionally, the scanning layer thickness can reach the micron level. This method can be used to segment and measure the tissue well under the condition of clearly preserving the internal structures of the sample, simplifying and increasing the accuracy of measuring tissue structures(12) .

In this study, a visually 3D reconstruction model was established based on micro-CT data and measurements. By measuring and analyzing the relationship between the stapes bone and surrounding structures in 15 cases, a simulated stapedotomy procedure through the external auditory canal was performed within the model. The possible influence and clinical significance of variation of the stapes and its surrounding structures on stapes surgery in otosclerosis were discussed.

MATERIALS AND METHODS

Materials and scanning methods

Fifteen (30 sides) adult cadaveric head specimens of Asian ethnicity (6 males and 9 females, aged 44 ± 8.67) were obtained and immersed in formalin for preservation and fixation. The bilateral temporal bones of the cadaveric head were cut and separated, and parts

including the complete external auditory canal, middle ear and inner ear were removed. The use of specimens in this study was approved by medical ethics committee of the First Affiliated Hospital of Guangxi Medical University (No. 2021KY-E-163). The specimens were numbered and labeled, and the separated temporal bones were scanned by micro-CT (skyscan 1176; Brucker, Belgium) (scanning parameters: tube current, 276 μ A; scanning layer thickness, 16 μ m; Scanning time, 285 ms; resolution, 1336 \times 2000). The obtained image was exported to a DCM format image for saving.

CT image reconstruction and measurement

The micro-CT images were imported into Mimics 20.0 software to reconstruct the complete structures of the ossicle, the horizontal segment of the facial nerve and the external auditory canal (as shown in Figures 1 and 2).

Using the reconstructed 3D model, the length, width and thickness of the stapes footplate and distance between the anterior and posterior crus of the stapes were measured (as shown in Figure 3).

Using the reconstructed 3D model, the distance between the stapes footplate and long process of the incus, angle of the incudostapedial joint, distance from the center of the stapes footplate to the horizontal segment of the facial canal, and distance from the horizontal segment of the facial canal to the plane of the stapes arch were measured. The path of stapedotomy through the external auditory canal was simulated, the posterior upper wall of the external auditory canal was removed, and the depth of the posterior upper wall of the external auditory canal to be removed was measured under the condition of exposing the incudostapedial joint, stapes footplate, part of the horizontal segment of the facial nerve, and the long process of the incus, malleus and other structures (as shown in Figures 4).

Statistical analysis

The measured data were input into SPSS statistical software for Windows (ver. 25.0; SPSS, Chicago, IL, USA) for processing and analysis, and the normality test was performed. Numerical variables with a normal distribution were expressed as means \pm standard

deviation, and comparisons between two groups were performed by paired t test. Nonparametric variables were represented as medians (P25, P75). Differences between two groups were analyzed by paired signed-rank test, with the test level of $p = 0.05$.

RESULTS

Reconstructions of the skull, skeleton, and facial nerve canal were completed for all 30 sides. No apparent abnormalities in the middle or inner ear were observed in any of the specimens. The measurement results related to the stapes footplate are presented in Table I, and a scatter plot is depicted in Figure 5. It was found that there were no significant differences in the values between males and females ($p > 0.05$), and the coefficients of variation among individuals were small, with almost no extreme outliers. Additionally, we measured the positional relationship between the stapes bone and surrounding tissue structures, and the results are presented in Table II, along with a scatter plot in Figure 6. It is important to note that "The distance between the stapes footplate and the long process of the incus" refers to the measurement taken with the starting point as the center of the stapes footplate. "The minimum depth of the external auditory canal required to remove" refers to the minimum depth of the posterior wall of the external auditory canal that needs to be eliminated, as measured in the simulated surgical model reconstructed using software. This depth must ensure visibility of the horizontal segment of the facial nerve, a portion of the long process of the incus where the piston hook is placed, as well as the overall view of the stapes bone. It was found that there were no significant differences in the values between males and females ($p > 0.05$). However, the measurements of both ears in one female sample showed significant deviations from the measurements of the other samples. Finally, we compared our partial measurement data with those reported by other researchers (Table III). Except for "The width of the stapes footplate", which showed a significant difference compared to the results of one researcher ($1.46 \pm 0.08 \text{mm}$ vs. $2.37 \pm 0.32 \text{mm}$), there were no major differences in the other measured values.

DISCUSSION

To date, many scholars have investigated the morphology and size of the stapes(13-16). However, the measurement results vary widely, and few reports have focused on the system of measurement. Additionally, these data are not necessarily consistent with findings in clinical practice and are not measured according to the operation reference point. Errors in measurements of the temporal bone may be caused by fixation and cutting of the specimen, limiting the use of many anatomical measurements in surgery(17).

In our study, we found that the measured results were consistent with those of Gu et al(16). However, there was a significant difference in "The width of the stapes footplate" compared to the results reported by Skinner et al(14). We believe that the source of this difference may be attributed to the variation in the racial composition of the selected samples. Some differences were found in the size of the auditory ossicles between different races, but further research is required to prove whether this hypothesis is correct. Furthermore, in previous studies, most of the measurements were based on fixed sections of temporal bone specimens after anatomy for routine anatomy or two-dimensional image measurement after plain CT scan, which may produce errors in the processing of specimen fixation and cutting, and the measurement of two-dimensional images may lead to inaccurate results due to scanning projection, which could also contribute to differences in measurement values.

In stapedotomy, the implanted piston can connect the auditory ossicles with the cochlear endolymph, causing the cochlear endolymph to vibrate and transmit sound waves to the inner ear(18). Carefully evaluating the location of the incus and stapes attachment to the piston is crucial during the operation. Although not all individual prostheses can be implanted perpendicular to the stapes footplate at an ideal angle of 90°, the tilting angle of the prosthesis from the direction normal to the stapes footplate was 30 degrees with a fenestration hole of 0.6-mm diameter, with little effect on prosthesis movement and hearing effects(19). In this study, we found that the angle of the incudostapedial joint was $88.29 \pm 11.58^\circ$ (73.97° - 121.82°). For most individuals, the angle between the incudostapedial joint has little effect on the postoperative effect. However, in a few individuals, a larger angle at the incudostapedial joint may potentially affect postoperative hearing recovery.

Presently, the diameter of most prostheses is 0.4 - 0.8 mm. Smaller-diameter prostheses

cannot better vibrate the lymph, affecting postoperative hearing improvement, while larger-diameter prostheses carry the risk of damaging the annular ligament of the stapes and causing the stapes footplate to float(20). In the present study, the width of the stapes footplate was 1.46 ± 0.08 mm (1.26 - 1.61 mm), which is much larger than the diameter of commonly used prostheses. Therefore, when drilling the stapes footplate at the correct position of the stapes footplate, it will not cause damage to the annular ligament of the stapes.

An inappropriate prosthesis size is an important cause of surgical failure, If the length of the prosthesis is too short, it may not be able to fully extend into the vestibule, leading to prosthesis displacement, causing erosion and wear of the prosthesis attachment point to the long process of the incus, and affecting postoperative hearing recovery(14). If the prosthesis is too long, the utricle and sacculus may be damaged, resulting in postoperative vertigo and even sensorineural hearing loss. Generally, the length of the implanted piston is equal to the distance from the long process of the incus to the stapes footplate, plus the thickness of the stapes footplate and length of the piston in the vestibule after passing through the stapes footplate. Presently, most scholars believe that the best piston depth should not exceed 0.5 mm(15, 21) . In the present study, the measured sum was approximately 4.6 mm, which can serve as a practical reference to select the prosthesis length in surgery (as shown in Figure 7).

Many reports worldwide have investigated the measurement of the relationships between the facial canal and its surrounding structures, but the selected positioning reference points are not standardized, leading to very different measurements. Zhu et al.(22) chose the stapes head as the positioning reference point, resulting in a shortest distance to the facial canal of 1.18 ± 0.42 mm. However, Wojciechowski et al.(23) selected the incudostapedial joint as the reference point, and the measured distance between the incudostapedial joint and horizontal segment of the facial nerve was 1.72 ± 0.33 mm. The position of perforation is considered close to the center of the stapes footplate, and the selection of this reference point is more consistent with the actual situation during the operation. To more realistically evaluate the actual anatomy during the operation, this study selected the reference distance as the distance from the center of the stapes floor to the facial nerve. Thus, the positional relationship between the center of the stapes footplate and the horizontal segment of the facial nerve canal

can be better clarified and more intuitively and accurately guide the protection of the facial nerve during the operation.

In the traditional procedure, a small perforation is first made in the footplate, and then the suprastructure of the stapes is removed; however, the process of perforation carries the risk of incus dislocation, stapes footplate fracture, stapes footplate floating and inner ear injury. In 1982, Fisch proposed a complete reversal of the procedural steps of classical stapedectomy(24). That is, before the suprastructure of the stapes is removed, perforation in the stapes footplate is made, and the piston is inserted. The suprastructure of the footplate is still connected to the long process of the incus, and the implanted piston can fix the stapes footplate during perforation to reduce the above risks. However, when a large range of lesions around the footplate or anatomical variations exist, such as drooping of the facial nerve, increasing the difficulty of exposing the stapes footplate, the operation will be more difficult using this method(25). Therefore, this method is not suitable for use in all stapes surgeries. Importantly, the anatomical characteristics of this region should be evaluated accurately to choose the method of operation. Many studies have shown that an implant diameter of 0.6 mm is the most suitable choice(26-28). Therefore, presently, the piston size most commonly used by ear surgeons is 0.6 mm. The distance between the horizontal segment of the facial canal and plane of the stapes arch can be used to evaluate whether the 0.6 mm perforated laser beam and piston can smoothly pass through the area between the suprastape structure and facial nerve without causing damage to the facial nerve before removing the suprastape structure. In this study, only 1 of the 15 specimens was found that the distance from the horizontal segment of the facial nerve to the plane of the stapes arch was less than 0.6mm (No. 10 specimen, 10L = 0.37mm, 10R = 0.48mm). It can be seen that In Fisch's stapedotomy, the use of a laser beam with a diameter of 0.6 mm applies to most patients.

To better expose the stapes footplate in stapedotomy for otosclerosis, it is often necessary to cut off part of the posterosuperior wall of the external auditory canal according to the actual situation. The external auditory canal generally has an "s" shaped(29), but its shape varies among individuals, and the thickness of the bone to be excavated during the surgical procedure also differs.(30). Roychaudhuri et al.(31) measured the distance of the overhang of

the posterosuperior bony canal wall required to be removed for adequate exposure of the incudostapedial complex during stapes surgery. They evaluated the thickness of the posterosuperior wall of the external auditory canal to be excised and divided it into four groups: A: 0-2 mm, B: 2-2.5 mm, C: 2.5-3 mm, D: > 3 mm. The thickness of the external auditory canal to be removed in most patients (55%) was in group B. In the standard stapes surgery for otosclerosis, part of the long process of the incus, stapedius muscle, pyramidal eminence and part of the horizontal segment of the facial nerve must be exposed. In the present study, the thickness of the posterior superior wall of the external auditory canal to be removed was 2.17 ± 0.91 mm, which was similar to that measured by Roychaudhuri. Micro-CT reconstruction was used to simulate the stapedotomy of otosclerosis through the external auditory canal. The head can be rotated arbitrarily according to the operation standard to adjust the optimal angle of the operation area, making the measurement method more intuitive and convenient. According to the above grouping, the thickness of the posterior superior wall of the external auditory canal to be removed was measured as 5.50 mm and 5.52 mm in 2 (6.67%) of the 30 specimens (2R and 2L), values much greater than 3 mm. Tang et al.(32) measured the shortest distance between the midpoint of the posterior wall of the external auditory canal and facial nerve as 3.37 ± 0.34 mm. When the posterior wall of the external auditory canal was cut deep, there was a risk of damaging the facial nerve and causing postoperative facial paralysis. In the measurement results of this study, for a small number of individuals, when the posterior wall of the external auditory canal is removed during the standard operation, there may be a risk of damaging the facial nerve that increases the difficulty of the operation; thus, preoperative assessment should be fully done. During the operation, the position of the facial nerve should be accurately evaluated according to the actual situation. The external auditory canal should not be chiseled blindly.

In this study, micro-CT images were used to measure the spatial relationship between stapes and their surrounding structures. On the one hand, it can more clearly and intuitively reflect the shape of stapes without damaging the accuracy of fine structure measurement; on the other hand, it also makes the structure of the stapes and surrounding surgical area better displayed. However, only 15 cadaveric head specimens were used in this study, which is

insufficient. We recommend that future studies focus on larger sample sizes to better understand stapes variation among different sexes, ages, and genetic backgrounds. Future studies are warranted to reconstruct more middle ear and inner ear structures, further explore the relationship between the stapes and saccule, utricle, chorda tympani nerve and peripheral blood vessels, and make the surgical area structure of the stapes clearer. Additionally, more factors must be comprehensively analyzed that affect the surgical operation and more practical references are required for otologists. Due to the limitations in specimen size, Micro-CT cannot be directly applied in clinical practice. In recent years, researchers have shown interest in the application of Cone Beam CT (CBCT) for measuring the ossicles and surrounding tissue structures(33). CBCT offers higher resolution compared to traditional CT and eliminates the sample size restrictions associated with Micro-CT. This makes CBCT potentially valuable for preoperative assessment in stapedotomy. Further research will be conducted to explore its potential in this regard.

CONCLUSIONS

A 3D model of the stapes bone and its surrounding anatomical structures was established based on Micro-CT imaging, and anatomical parameters of the stapes bone and its surrounding structures were measured using the model. Based on these data, we recommend an implanted piston diameter of 0.6mm and a length of approximately 4.6mm for stapedotomy. We found that the distance from the center of the stapes footplate to the facial nerve was 1.60 ± 0.34 mm, highlighting the need for special attention to the position of the facial nerve during the procedure. Lastly, we measured the thickness of the excised posterior superior wall of the external auditory canal, which needs to be removed during stapedotomy, to be 2.17 ± 0.91 millimeters, providing anatomical references for otologists.

Acknowledgements

Dr. Gong L. is responsible for the overall execution of the experiment; Dr. Feng Y.W. created pictures and tables; Dr. Tang X.L. completed the operation of micro-CT; Dr. Zhou W.W. is responsible for data statistics; Prof. Tan S.H. and Prof. Tang A.Z. designed this

experiment and provided guidance on the key steps. This research was funded by the Natural Science Foundation of China (grant number 32060132 and U21A20371). No conflict of interest exists in this research.

Conflict of interest: None declared

XREFERENCES

1. Nazarian R, McElveen JT, Jr., Eshraghi AA. History of Otosclerosis and Stapes Surgery. *Otolaryngologic clinics of North America*. 2018;51(2):275-90. Epub 2018/03/06. doi: 10.1016/j.otc.2017.11.003. PubMed PMID: 29502722.
2. Quesnel AM, Ishai R, McKenna MJ. Otosclerosis: Temporal Bone Pathology. *Otolaryngologic clinics of North America*. 2018;51(2):291-303. Epub 2018/02/06. doi: 10.1016/j.otc.2017.11.001. PubMed PMID: 29397947.
3. Cureoglu S, Baylan MY, Paparella MM. Cochlear otosclerosis. *Current opinion in otolaryngology & head and neck surgery*. 2010;18(5):357-62. Epub 2010/08/10. doi: 10.1097/MOO.0b013e32833d11d9. PubMed PMID: 20693902; PubMed Central PMCID: PMC3075959.
4. de Oliveira Penido N, de Oliveira Vicente A. Medical Management of Otosclerosis. *Otolaryngologic clinics of North America*. 2018;51(2):441-52. Epub 2018/03/06. doi: 10.1016/j.otc.2017.11.006. PubMed PMID: 29502728.
5. Bartel R, Sanz JJ, Clemente I, Simonetti G, Viscacillas G, Palomino L, et al. Endoscopic stapes surgery outcomes and complication rates: a systematic review. *Eur Arch Otorhinolaryngol*. 2021;278(8):2673-9. Epub 2020/10/02. doi: 10.1007/s00405-020-06388-8. PubMed PMID: 33001293.
6. Cheng HCS, Agrawal SK, Parnes LS. Stapedectomy Versus Stapedotomy. *Otolaryngologic clinics of North America*. 2018;51(2):375-92. Epub 2018/02/06. doi: 10.1016/j.otc.2017.11.008. PubMed PMID: 29397948.
7. Srivastava R, Cho W, Fergie N. The Use of Lasers in Stapes Surgery. *Ear, nose, & throat journal*. 2021;100(1_suppl):73s-6s. Epub 2020/07/01. doi: 10.1177/0145561320937828. PubMed PMID: 32603217.

8. Benson JC, Carlson ML, Lane JJ. MRI of the Internal Auditory Canal, Labyrinth, and Middle Ear: How We Do It. *Radiology*. 2020;297(2):252-65. Epub 2020/09/23. doi: 10.1148/radiol.2020201767. PubMed PMID: 32960730.
9. Haußmann A, Yilmaz U. Anatomy of the petrous portion of the temporal bone. *Der Radiologe*. 2019;59(12):1058-63. Epub 2019/11/11. doi: 10.1007/s00117-019-00606-z. PubMed PMID: 31705161.
10. Ahmad N, Wright A. Three-dimensional temporal bone reconstruction from histological sections. *The Journal of laryngology and otology*. 2014;128(5):416-20. Epub 2014/05/29. doi: 10.1017/s0022215114000917. PubMed PMID: 24865375.
11. Gielkens PF, Schortinghuis J, de Jong JR, Huysmans MC, Leeuwen MB, Raghoobar GM, et al. A comparison of micro-CT, microradiography and histomorphometry in bone research. *Archives of oral biology*. 2008;53(6):558-66. Epub 2008/01/15. doi: 10.1016/j.archoralbio.2007.11.011. PubMed PMID: 18190892.
12. Kaftan H, Böhme A, Martin H. Geometric parameters of the ossicular chain as a function of its integrity: a micro-CT study in human temporal bones. *Otology & neurotology : official publication of the American Otological Society, American Neurotology Society [and] European Academy of Otology and Neurotology*. 2015;36(1):178-83. Epub 2014/04/03. doi: 10.1097/mao.0000000000000315. PubMed PMID: 24691506.
13. Sim JH, Rösli C, Chatzimichalis M, Eiber A, Huber AM. Characterization of stapes anatomy: investigation of human and guinea pig. *Journal of the Association for Research in Otolaryngology : JARO*. 2013;14(2):159-73. Epub 2013/01/10. doi: 10.1007/s10162-012-0369-5. PubMed PMID: 23299488; PubMed Central PMCID: PMC3660917.
14. Skinner M, Honrado C, Prasad M, Kent HN, Selesnick SH. The incudostapedial joint angle: implications for stapes surgery prosthesis selection and crimping. *The Laryngoscope*. 2003;113(4):647-53. Epub 2003/04/03. doi: 10.1097/00005537-200304000-00012. PubMed PMID: 12671422.
15. Takahashi H, Sando I. Three-dimensional surgical anatomy for stapes surgery computer-aided reconstruction and measurement. *The Laryngoscope*. 1992;102(10):1159-64. Epub 1992/10/01. doi: 10.1288/00005537-199210000-00011. PubMed PMID: 1405967.

16. Yuyan G, Dongdong R, Chao H. Significance of the measurement of normal Chinese adult stapes. *Chinese Journal of Ophthalmology and Otorhinolaryngology*. 2017;17(01):16-8. doi: 10.14166/j.issn.1671-2420.2017.01.005.
17. Dahm MC, Shepherd RK, Clark GM. The postnatal growth of the temporal bone and its implications for cochlear implantation in children. *Acta oto-laryngologica Supplementum*. 1993;505:1-39. Epub 1993/01/01. PubMed PMID: 8379315.
18. Sevy A, Arriaga M. The Stapes Prosthesis: Past, Present, and Future. *Otolaryngologic clinics of North America*. 2018;51(2):393-404. Epub 2018/03/06. doi: 10.1016/j.otc.2017.11.010. PubMed PMID: 29502725.
19. Cuny P, Alsolami NJ, Dobrev I, Warnholtz B, Rösli C, Sim JH. Influence of angular positioning of the prosthesis in stapes surgeries with a NiTiBond prosthesis: Investigation in cadaveric temporal bones. *Hearing research*. 2019;378:149-56. Epub 2019/01/22. doi: 10.1016/j.heares.2019.01.005. PubMed PMID: 30661818.
20. Gristwood RE, Venables WN. Effects of fenestra size and piston diameter on the outcome of stapes surgery for clinical otosclerosis. *The Annals of otology, rhinology, and laryngology*. 2011;120(6):363-71. Epub 2011/07/22. doi: 10.1177/000348941112000603. PubMed PMID: 21774442.
21. Backous DD, Minor LB, Aboujaoude ES, Nager GT. Relationship of the utriculus and sacculus to the stapes footplate: anatomic implications for sound-and/or pressure-induced otolith activation. *The Annals of otology, rhinology, and laryngology*. 1999;108(6):548-53. Epub 1999/06/23. doi: 10.1177/000348949910800604. PubMed PMID: 10378521.
22. Zhu F, Sun M, Zhang J, Sun D, Jiang Y. Location of tympanic segment and mastoid segment of facial nerve and prevention of prosopoplegia in operations. *Lin chuang er bi yan hou tou jing wai ke za zhi = Journal of clinical otorhinolaryngology, head, and neck surgery*. 2011;25(7):314-6. Epub 2011/06/30. PubMed PMID: 21710720.
23. Wojciechowski T, Skadorwa T, Nève de Mévergnies JG, Niemczyk K. Microtomographic morphometry of the stapedius muscle and its tendon. *Anatomical science international*. 2020;95(1):31-7. Epub 2019/05/22. doi: 10.1007/s12565-019-00490-6. PubMed PMID: 31111392; PubMed Central PMCID: PMC6942563.

24. Ueda H, Kishimoto M, Uchida Y, Sone M. Factors affecting fenestration of the footplate in stapes surgery: effectiveness of Fisch's reversal steps stapedotomy. *Otology & neurotology* : official publication of the American Otological Society, American Neurotology Society [and] European Academy of Otology and Neurotology. 2013;34(9):1576-80. Epub 2013/10/19. doi: 10.1097/MAO.0b013e3182a473eb. PubMed PMID: 24136325.
25. Malafrente G, Filosa B. Fisch's reversal steps stapedotomy: when to use it? *Otology & neurotology* : official publication of the American Otological Society, American Neurotology Society [and] European Academy of Otology and Neurotology. 2009;30(8):1128-30. Epub 2009/10/10. doi: 10.1097/MAO.0b013e3181be686e. PubMed PMID: 19816228.
26. Bernardeschi D, De Seta D, Canu G, Russo FY, Ferrary E, Lahlou G, et al. Does the diameter of the stapes prosthesis really matter? A prospective clinical study. *The Laryngoscope*. 2018;128(8):1922-6. Epub 2017/11/25. doi: 10.1002/lary.27021. PubMed PMID: 29171673.
27. Marchese MR, Cianfrone F, Passali GC, Paludetti G. Hearing results after stapedotomy: role of the prosthesis diameter. *Audiology & neuro-otology*. 2007;12(4):221-5. Epub 2007/03/29. doi: 10.1159/000101329. PubMed PMID: 17389788.
28. Sennaroğlu L, Unal OF, Sennaroğlu G, Gürsel B, Belgin E. Effect of teflon piston diameter on hearing result after stapedotomy. *Otolaryngology--head and neck surgery* : official journal of American Academy of Otolaryngology-Head and Neck Surgery. 2001;124(3):279-81. Epub 2001/03/10. doi: 10.1067/mhn.2001.112431. PubMed PMID: 11240991.
29. Grewe J, Thiele C, Mojallal H, Raab P, Sankowsky-Rothe T, Lenarz T, et al. New HRCT-based measurement of the human outer ear canal as a basis for acoustical methods. *American journal of audiology*. 2013;22(1):65-73. Epub 2012/10/16. doi: 10.1044/1059-0889(2012/12-0039). PubMed PMID: 23064418.
30. Yu JF, Lee KC, Wang RH, Chen YS, Fan CC, Peng YC, et al. Anthropometry of external auditory canal by non-contactable measurement. *Applied ergonomics*. 2015;50:50-5. Epub 2015/05/12. doi: 10.1016/j.apergo.2015.01.008. PubMed PMID: 25959317.
31. Roychaudhuri BK, Roychowdhury A, Ghosh S, Nandy S. Study on the anatomical

variations of the posterosuperior bony overhang of external auditory canal. Indian journal of otolaryngology and head and neck surgery : official publication of the Association of Otolaryngologists of India. 2011;63(2):136-40. Epub 2012/04/03. doi: 10.1007/s12070-010-0101-x. PubMed PMID: 22468249; PubMed Central PMCID: PMC3102168.

32. Tang YK, He G, Fan JG, Zhu W. The study of locating facial nerve precisely in middle ear surgery based on clinical anatomy. J Clin Otorhinolaryngol Head Neck Surg. 2017;31(17):1334-7. Epub 2018/05/26. doi: 10.13201/j.issn.1001-1781.2017.17.009. PubMed PMID: 29798225.

33. Wojciechowski T, Skadorwa T, Fermi M, Szopiński K. Radiologic evaluation and clinical assessment of facial sinus in adults and children - computed tomography study. Auris, nasus, larynx. 2023. Epub 2023/06/18. doi: 10.1016/j.anl.2023.06.003. PubMed PMID: 37330319.

Table I. Measurements of stapes footplate parameters

| | Total (n=30) | Male (n=12) | Female(n=18) | <i>p</i> | RI |
|---|--------------|-------------|--------------|----------|-----------|
| The length of stapes footplate [mm] | 2.93±0.17 | 2.97±0.22 | 2.90±0.13 | 0.537 | 2.87-3.00 |
| The width of the stapes footplate [mm] | 1.46±0.08 | 1.45±0.06 | 1.46±0.09 | 0.945 | 1.43-1.50 |
| The distance between the anterior and posterior crus of the stapes [mm] | 1.65±0.28 | 1.75±0.20 | 1.58±0.30 | 0.066 | 1.55-1.75 |
| The thickness of the stapes footplate [mm] | 0.30±0.11 | 0.32±0.09 | 0.28±0.12 | 0.568 | 0.26-0.34 |

p >0.05: considered to be no significantly different. RI was calculated using the 2.5th and 97.5th percentiles.

Table II. Measurements of relationships between the stapes and surrounding structures.

| | Total (n=30) | Male (n=12) | Female(n=18) | p | RI |
|---|---------------------|--------------------|---------------------|----------|-------------|
| The distance between the stapes footplate and the long process of the incus [mm] | 3.79±0.39 | 3.75±0.31 | 3.82±0.44 | 0.631 | 3.65-3.94 |
| The angle of the incudostapedial joint [°] | 88.29±11.58 | 82.31±8.00 | 92.28±12.05 | 0.11 | 83.97-92.62 |
| The distance from the center of the stapes footplate to the facial canal (mm) | 1.60±0.34 | 1.63±0.25 | 1.58±0.37 | 0.802 | 1.47-1.73 |
| The distance from the horizontal segment of the facial canal to the plane of the stapes arch (mm) | 1.05±0.31 | 1.11±0.21 | 1.01±0.36 | 0.302 | 0.93-1.17 |
| The minimum depth of the external auditory canal required to remove (mm) | 2.17±0.91 | 1.93±0.47 | 2.33±1.09 | 0.723 | 1.83-2.51 |

p >0.05: considered to be no significantly different. RI was calculated using the 2.5th and 97.5th percentiles.

Table III. Comparison of human stapes dimension with data in the literature (mean±standard deviation)

| | Present data | Takahashi and Sando (17) | Skinner et al. (16) | Sim et al. (15) | Gu and Dongdong (18) |
|---|---------------------|---------------------------------|----------------------------|------------------------|-----------------------------|
| The length of stapes footplate | 2.93±0.17 | - | 3.60±0.495 | 2.81±0.158 | 2.89± 0.15 |
| The width of the stapes footplate | 1.46±0.08 | - | 2.37±0.32 | 1.27±0.109 | 1.42 ± 0.09 |
| The distance between the stapes footplate and the long process of the incus | 3.79±0.39 | 3.80±0.28 | - | - | - |
| the angle of the incudostapedial joint | 88.29±11.58 | - | 93.0±8.27 | - | - |
| n | 30 | 9 | 13 | 53 | 12 |

Figure 1. The 2D image of stapes was obtained by micro-CT scanning. (A) and (B) shows the length and width of stapes footplate; (C) shows the thickness of the stapes footplate and the distance between the anterior and posterior crus of the stapes. Abbreviations: CC, cochlea; EAC, external auditory canal; IC, incus; ST, stapes, TB, temporal bone; VT, vestibule.

Figure 2. The 2D image of stapes was obtained by micro-CT scanning. (A) shows the angle of the incudostapedial joint; (B) shows the distance between the stapes footplate and the long process of the incus; (C) shows the distance from the center of the stapes footplate to the facial canal and the distance from the horizontal segment of the facial canal to the plane of the stapes arch. Abbreviations: CC, cochlea; EAC, external auditory canal; FN, facial nerve; IC, incus; ST, stapes, TB, temporal bone; VT, vestibule.

Figure 3. The 3D image of stapes was obtained by micro-CT scanning.

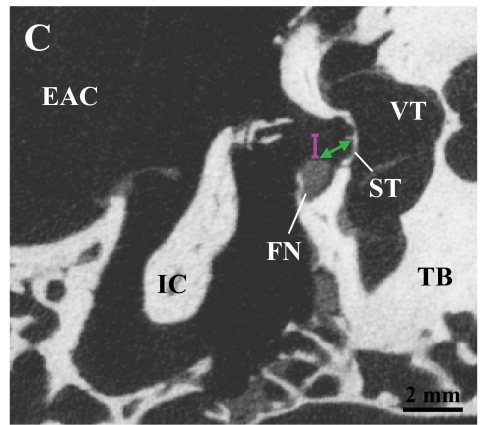
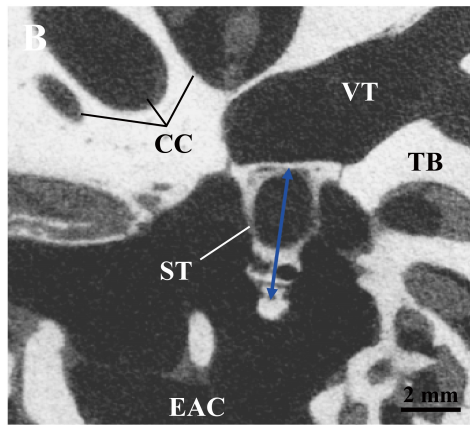
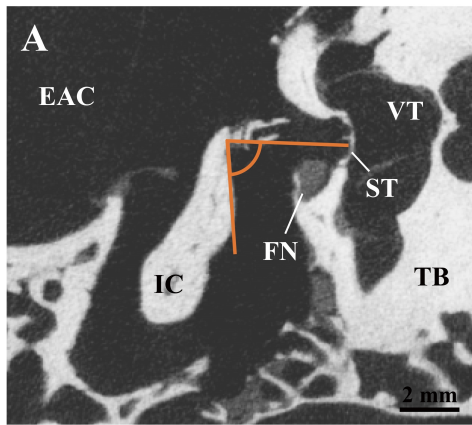
Figure 4. The 3D image of stapes was obtained by micro-CT scanning. (A) and (B) show the spatial relationship between the stapes and the incus; (C), (D) and (E) show the spatial relationship between the stapes and the facial nerve. (F) shows the minimum depth of the external auditory canal required to remove. Abbreviations: EAC, external auditory canal; FN, facial nerve, MA, malleus; IC, incus; ST, stapes; STM, Stapedius muscle.

Figure 5. Scatter diagram of data distribution. (A) Distribution of the length of stapes footplate; (B) Distribution of the width of stapes footplate; (C) Distribution of the distance between the anterior and posterior crus of the stapes; (D) Distribution of the thickness of stapes footplate.

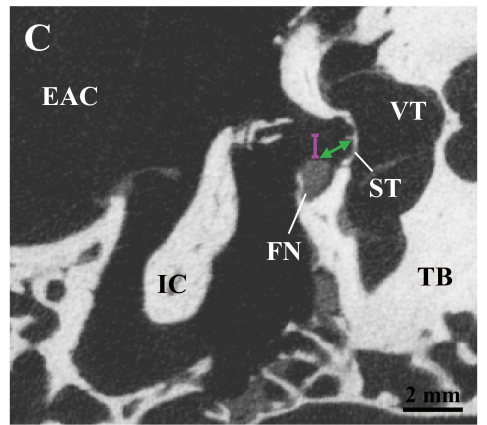
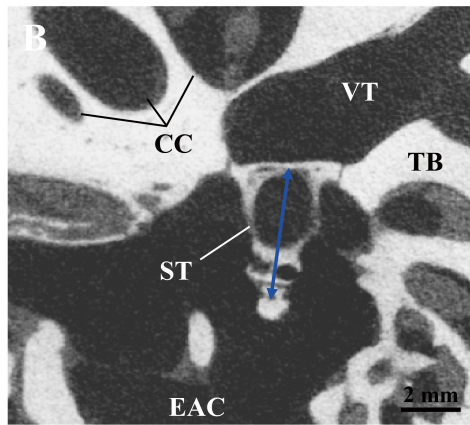
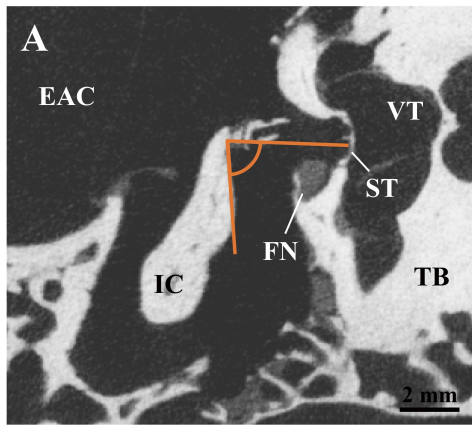
Figure 6. Scatter diagram of data distribution. (A) Distribution of the distance between the stapes footplate and the long process of the incus. (B) Distribution of the angle of the incudostapedial joint. (C) Distribution of the distance from the center of the stapes footplate

to the facial canal. (D) Distribution of the distance from the horizontal segment of the facial canal to the plane of the stapes arch. (E) The minimum depth of the external auditory canal required to remove (mm)

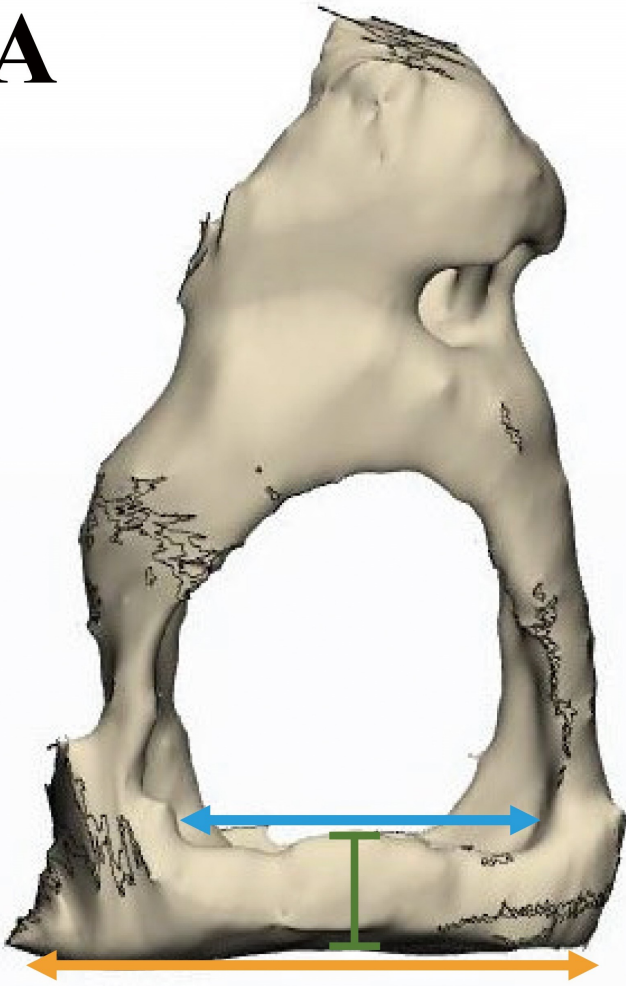
Figure 7. Calculation of the length of implanted piston. The distance between the stapes footplate and the long process of the incus is approximately equal to 3.8 mm; the thickness of the stapes footplate is approximately equal to 0.3 mm, and the best piston depth should not exceed 0.5 mm, so the measured sum was approximately 4.6 mm.



-  The angle of the incudostapedial joint
-  The distance between the stapes footplate and the long process of the incus
-  The distance from the center of the stapes footplate to the facial canal
-  The distance from the horizontal segment of the facial canal to the plane of the stapes arch



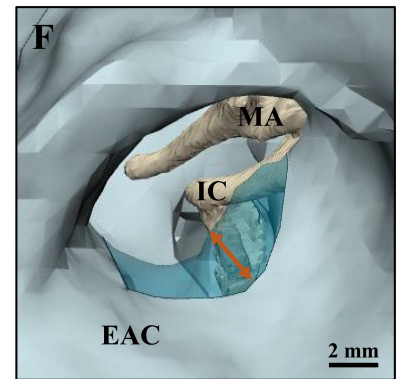
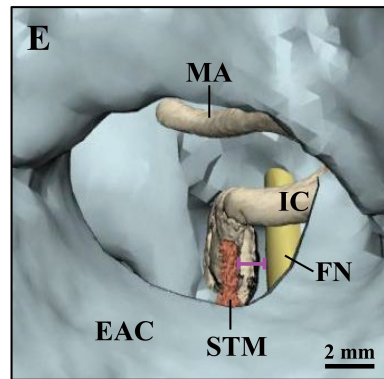
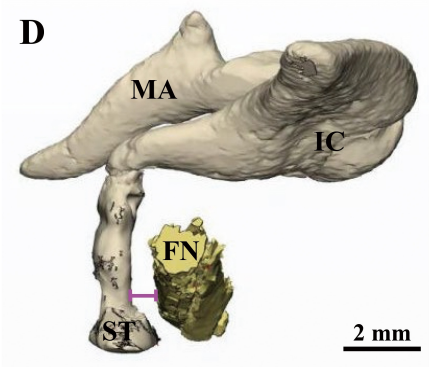
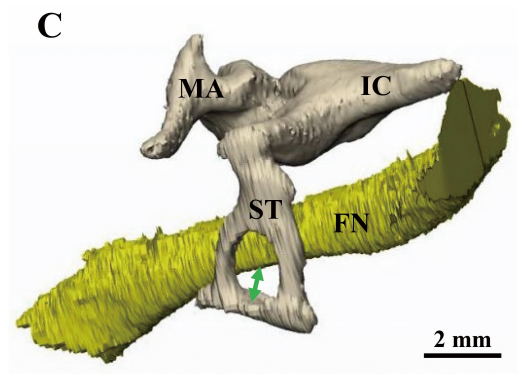
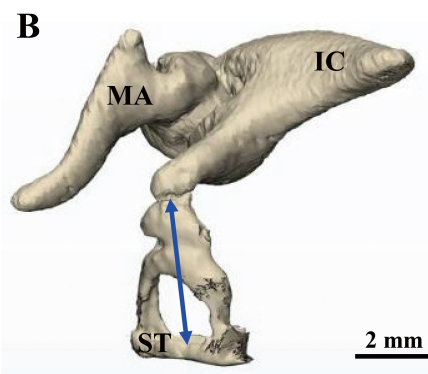
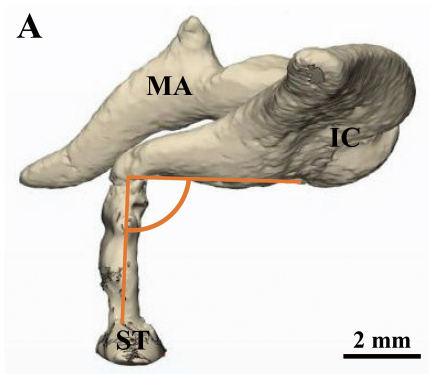
-  The angle of the incudostapedial joint
-  The distance between the stapes footplate and the long process of the incus
-  The distance from the center of the stapes footplate to the facial canal
-  The distance from the horizontal segment of the facial canal to the plane of the stapes arch

A**B**

↔ The length of stapes footplate — The thickness of the stapes footplate

↔ The distance between the anterior and posterior crus of the stapes

↔ The width of the stapes footplate



-  The angle of the incudostapedial joint  The distance between the stapes footplate and the long process of the incus
-  The distance from the center of the stapes footplate to the facial canal
-  The distance from the horizontal segment of the facial canal to the plane of the stapes arch
-  The minimum depth of the external auditory canal required to remove

